ADVANCED QUANTUM TECHNOLOGIES
www.advquantumtech.com

Large Spontaneous Emission Enhancement with Silver Nanocube Dimers on Silver Substrates

Yinhui Kan, Sergey I. Bozhevolnyi, and Shailesh Kumar**

Nanoantennas and nanocavities are widely used for at-source manipulation of quantum emission based on the well-known Purcell effect. Here, the configuration is explored consisting of silver (Ag) nanocube dimers positioned on Ag substrates to realize large Purcell enhancement of molecular spontaneous emission. The relationship is investigated between the cube sizes and separation gap of a nanocube dimer and the resulting Purcell enhancement, and shows the possibility of achieving the enhancement of up to 6.4×10^6. Furthermore, to experimentally demonstrate large Purcell enhancements, atomic force microscopy is used to assemble Ag nanocube dimers in the corner-to-corner configuration with the help of prefabricated corner-to-corner dielectric bricks. The decrease of the lifetime of Ru dye molecules from 91.7 ns (on a glass substrate) to the instrument response function limit (1.5 ns) after coupling with nanocube dimers is observed. This work provides a promising design and realization method for advanced photon sources, e.g., atom-like single-photon emitters with extremely large decay rates.

1. Introduction

Spontaneous emission (SE) is one of the fundamental processes for generating single photons that are crucial for modern optics and relevant applications, such as quantum communications, sensing, and computing.[1–5] The SE rates of quantum emitters (QEs) are not only determined by QEs themselves but also by the surrounding (nanostructured) environment as a result of the Purcell effect.[6–8] Owing to this effect, the photon emission can be tailored at source by coupling with carefully designed nanostructures to overcome the intrinsic problems of most standalone (i.e., in homogenous environment) QEs, including quantum dots, molecules, and defect centers in diamonds, featuring low emission rates and efficiency, that prevent them from being directly used in advanced optical technologies.[9–13] Generally, the SE rates can be significantly increased with the QEs being placed in engineered environments with the increased local density of optical states. The latter can be realized with different kinds of micro/nano structures made of either dielectric or metallic (or hybrid) materials that have been designed as nanoantennas and nanocavities in the last decade.[14–17]

The SE rate enhancement for QEs coupled with micro/nano structures with respect to that in free space is normally characterized by the Purcell factor, which is proportional to the ratio between the quality factor and mode volume of the resonant micro/nano structures.[18–20] It has been established that dielectric cavities show limited SE rate enhancements because of the diffraction limit imposed on the cavity size and the slow out-of-cavity emission for cavities with too large quality factors.[21,22] On the contrary, plasmonic nanocavities are not subjected to the diffraction limit and thus can be made extremely small. This opens the possibility for realizing extremely large SE enhancements, even in the presence of inevitable absorption losses. Configurations like nanospheres,[23,24] nanowires,[25,26] V grooves,[27] and recently developed metasurfaces have been applied to increase the SE rate.[28,29] Some of the latter configurations allow one to also go beyond the SE rate enhancement and engineer the SE directionality and polarization.[30–33] Plasmonic antennas featuring small gaps have been proposed and utilized for obtaining large fluorescence enhancements. Bowtie antennas were utilized for obtaining single molecule fluorescence enhancements of up to 1340.[34] Metal nanoparticles (nanocubes or nanobricks) on top of metal films (NPoM) with small dielectric nanogaps, have been demonstrated as another promising configuration to enhance the SE rate for molecules,[35,36] quantum dots,[37,38] and color centers in nanodiamonds.[39] High Purcell factors have been theoretically obtained for some of the NPoM structures.[19,40–42] For example, for a gold nanosphere placed on a gold mirror with a 0.9 nm gap, the Purcell factor obtained was $\approx 3 \times 10^6$.[40] In experiments, with NPoM configuration a fluorescence enhancement larger than 30 000 was reported,[36] and in a similar configuration Purcell enhancements of ≈ 2000 was obtained.[35] Although dimer antennas have been proposed before with different variations including bowties[34,43] and cube dimers,[44] the realization of extremely high Purcell enhancements with reliable

Y. Kan, S. I. Bozhevolnyi, S. Kumar
Center for Nano Optics
University of Southern Denmark
Odense M DK-5230, Denmark
E-mail: seib@mci.sdu.dk; shku@mci.sdu.dk

The ORCID identification number(s) for the author(s) of this article can be found under https://doi.org/10.1002/qute.202300196

DOI: 10.1002/qute.202300196

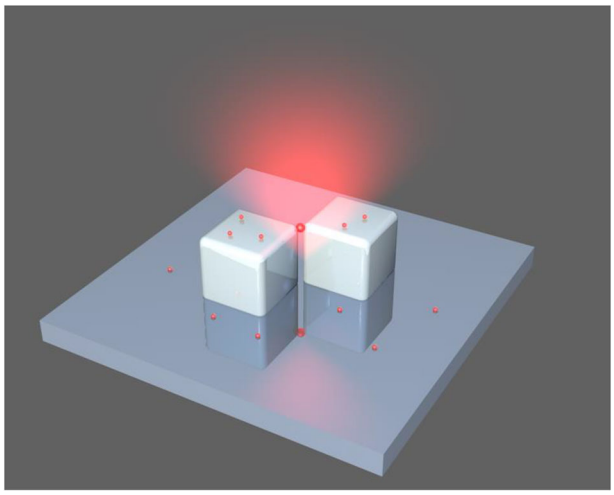

Figure 1. Schematic of an Ag nanocube dimer on a silver coated substrate coupled to Ru dye molecules resulting in large Purcell enhancement of molecular spontaneous emission.

experimental method remains elusive and intensively sought after.

In this work, we use silver (Ag) cube dimers on Ag-coated substrates to form nanoscale cavities enabling large Purcell enhancements. Ag-coated substrates help in reducing the gap mode volume and further enhance the SE rate when compared to Ag cube dimers on dielectric substrates.[26,45] We investigate the relationship between the cube sizes and separation gap and the resulting Purcell enhancement for QEs with their radiative dipoles oriented along the nanodimer gap. It is found that the Purcell enhancement of up to 6.4×10^6, is feasible. To experimentally demonstrate large Purcell enhancements, we use an atomic force microscope (AFM) to move Ag cubes forming corner-to-corner dimers with the help of prefabricated corner-to-corner polymer (HSQ) bricks. Ru dye molecules [(bis(2,2′-bipyridine)−4,4′-dicarboxybipyridine-ruthenium di (N-succinimidyl ester) bis(hexafluorophosphate)], which have a relatively long lifetime in visible frequency, are used to demonstrate the Purcell enhancements with the lifetime decrease from 91.7 ns (on a glass substrate) to the instrument response function limit (1.5 ns) after coupling with the designed Ag cube dimers.

2. Results and Discussion

Figure 1a shows a schematic of the considered configuration consisting of Ru dye molecules coupled with an Ag nanocube dimer located on a 150-nm-thick Ag film (a silicon substrate supporting the dimer-film arrangement is not shown). Two Ag nanocubes are arranged in a corner-to-corner configuration, forming thereby a nanoscale gap. In this work, we use Ru dye molecules with the emission peak at ≈630 nm when driven by an excitation laser (532 nm). The fluorescent molecules located at the top edge of the gap, where the local density of state is large, whose SE rates are expected to be significantly enhanced due to efficient coupling to a strongly confined plasmonic gap mode. Due to the Purcell enhancement, the molecules inside the gap emit photons faster than those located at other areas, thus dominating the total photon emission being collected in the far-field. It should be noted that the Purcell enhancement is maximized for the QEs having their radiative dipoles oriented (parallel to the prevailing electric field component of the plasmonic gap mode.[10]

As shown in **Figure 2**, the coupled system consists of two Ag cubes of the same size with an edge length L that are placed in a corner-to-corner configuration separated by a gap d. For simplicity, in this work, the cube orientation θ is fixed at 45°. The QE (i.e., Ru dye molecule) is modeled as a horizontal electric dipole placed in the middle of the gap d with a height h, at the top edge of the cubes (i.e., $h = L$). Nanocube dimer together with QE is immersed in a thin (200 nm) silica (SiO_2) film as shown in Figure 2b. The simulations are conducted utilizing 3D finite-difference time-domain (FDTD) method. We define the Purcell factor as $P_f = (\gamma_{rad} + \gamma_{nr})/\gamma_0$ and the quantum efficiency (QE_{ff}) as $QE_{ff} = \gamma_{rad}/\gamma_{tot}$, where γ_{rad} and γ_{nr} are the decay rates of radiative and nonradiative channels in the system with antenna structures, respectively; $\gamma_{tot} = \gamma_{rad} + \gamma_{nr}$ is the total decay rate; γ_0 is the decay rate of the emitter in the vacuum (we disregard the intrinsic nonradiative dissipation in the emitter, and the emitter is treated as an electric dipole in the simulation). We then calculate the influence of the cube size and gap distance on the Purcell factor and QE_{ff}. With a fixed dimer gap of $d = 1$ nm, we first analyze the influence of the cube size on the Purcell enhancement. As can be seen in Figure 2c, the Purcell factor is very large for a broad range of wavelengths and for different sizes of cubes with L ranging from 20 to 100 nm. Large Purcell enhancements are obtained in a broad spectral range, because the quality factor of these (plasmonic) cavities is low ≈10. For bigger cube sizes, we are away from cavity resonance and the enhancements are obtained mainly due to the confinement of the field in the gap of the cube dimer. For $L = 20$ nm, the Purcell factor reached 4.8×10^6 at the wavelength 623 nm. Considering Ru dye molecules with the emission peak at ∼ 630 nm, the optimal cube size is $L = 22$ nm with the Purcell factor reaching 6.4×10^6 (the line is not plotted).[23,24,35–39] In our experiment, we focus on the cube size with $L = 100$ nm, which can give a broadband and relatively large Purcell factor ($\approx 1 \times 10^6$), though it is not as large as that for the optimum cube size with $L = 22$ nm. It is easily understood that with an increase in the gap d, the Purcell factor would decrease, as illustrated in Figure 2d. However, with a gap $d = 10$ nm, the Purcell factor can still be larger than 1×10^3. As shown in Figure 2e, we can see the effect of cube size on QE_{ff} for a fixed gap distance $d = 1$ nm. We observe that QE_{ff} can be resonantly enhanced at the wavelength of 680 nm and cubes with $L = 50$ nm, while the cubes with $L = 100$ nm are overall most efficient. This is due to higher scattering efficiency of larger cubes. We define SE enhancement (radiative part) as a product of Purcell factor and QE_{ff}. For $L = 100$ nm, the SE enhancement (3.5×10^4) is larger than those obtained for smaller cube sizes. With an increase in the gap distance, the SE enhancement decreases, even though the quantum efficiency QE_{ff} increases, resulting in various possibilities for the performance optimization. We also note that the observed photon count rate depends on the collection efficiency as well as the optical set-up used for the collection and detection of photons.

To experimentally demonstrate the large Purcell enhancement, we arrange Ag cube dimers using an AFM and deposit Ru dye molecules (with the size of 0.9 nm[47]) in the gap of the cube

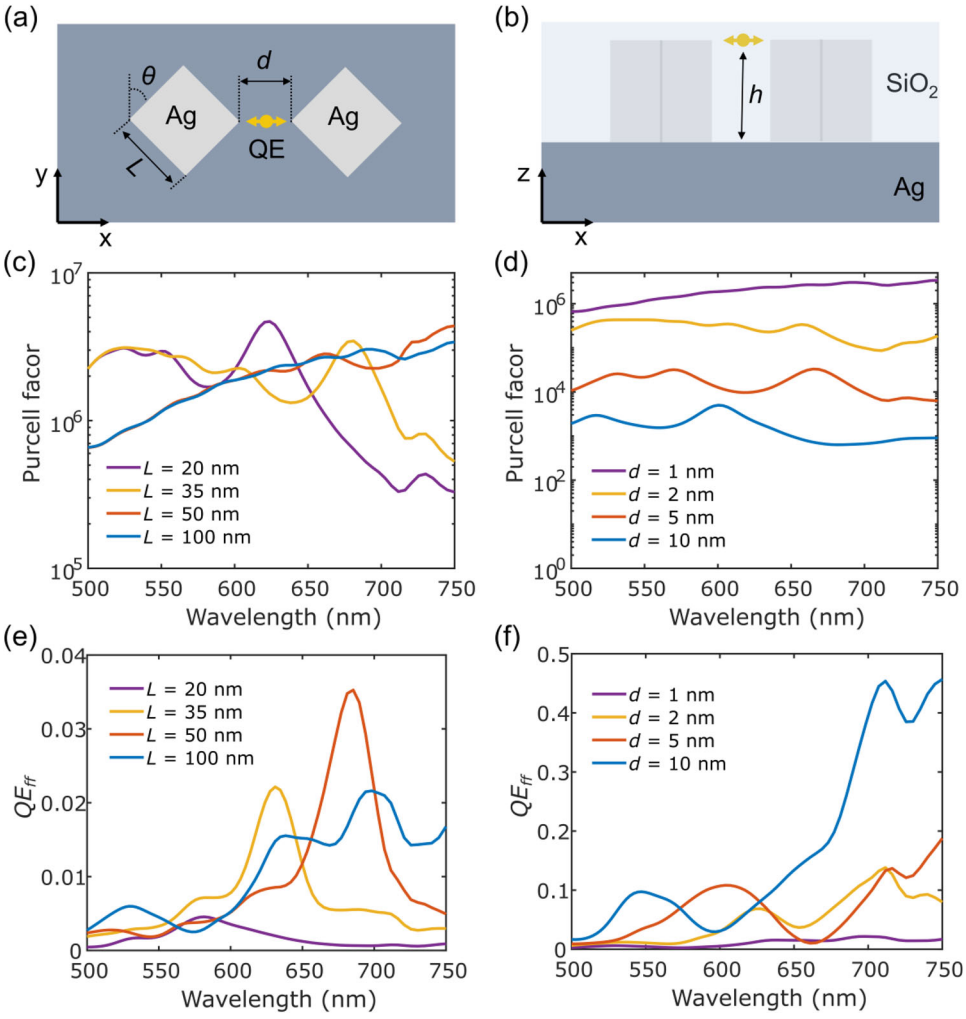

Figure 2. Purcell enhancement of a QE in a nanocavity built with corner-to-corner Ag nanocube dimer. a) Top view of the QE coupled Ag nanocube dimer configuration. b) Cross section view of the configuration. c) Relationship between the Purcell enhancement and the cube size, the gap distance is fixed at $d = 1$ nm. d) Relationship between the Purcell enhancement and the gap distance, the cube size is fixed with the side length of 100 nm. e) Relationship between the quantum efficiency QE_{ff} and the cube size, the gap distance is fixed at $d = 1$ nm. f) Relationship between QE_{ff} and the gap distance, the cube size is fixed with the side length of 100 nm. The height of emitter is fixed at the top edge of the cube (i.e., $h = L$).

dimer. The fabrication process is illustrated in **Figure 3**. First, a 150 nm thick Ag film is deposited on a Si Wafer, which is used as the substrate. We then spin-coat hydrogen silsesquioxane (HSQ) (refractive index = 1.41) film with a thickness of 150 nm.[31] HSQ brick dimers are fabricated with edge lengths of 100 nm and a separation of ≈10 nm. HSQ brick dimers are used to catch Ag cubes in the spin-coating process and to further utilize them in the moving process of Ag cubes using AFM, to assemble the Ag cube dimers. The Ag cubes found within a short distance, that is, nearby HSQ bricks were moved by the AFM tip to form cube dimers in a corner-to-corner configuration, following the process illustrated in detail in our previous work.[44] Ru dye molecules are then spin-coated on the samples, which results in some of the molecules getting placed in the gap of Ag cube dimers.

Figure 4 illustrates the fabrication and assembling process of Ag cube dimers. Figure 4a shows a dark-field microscope image of an area (100 × 100 μm) with fabricated HSQ markers and bricks. The markers are used to build a coordinate system and are used to determine the position of cube dimers. The solution containing Ag cubes with a proper concentration is spin-coated on the surface, on which the cubes are randomly and almost evenly distributed (Figure 4b). Most of the cubes on the substrate are separate, while some cubes get conjoined as cube dimers even without moving with the AFM (Figure 4c). As shown in Figure 4d,e, for the cubes near the HSQ bricks, we can use AFM to move the cubes close to the HSQ bricks. Once two Ag cubes are placed at the corner of the HSQ brick dimer, they form the Ag cube dimer as expected (Figure 4f).

The Ru dye molecules are excited by a 532 nm linearly polarized pulsed laser. In this work, we mainly focused on the decay rate (lifetime) of Ru dye molecules, the concentration of molecular solution and the intensity of pulsed laser (spot size is about 0.5 μm) were differently adjusted in different cases to obtain sufficient photon counts (≈20 kcps) for the decay rate measurement

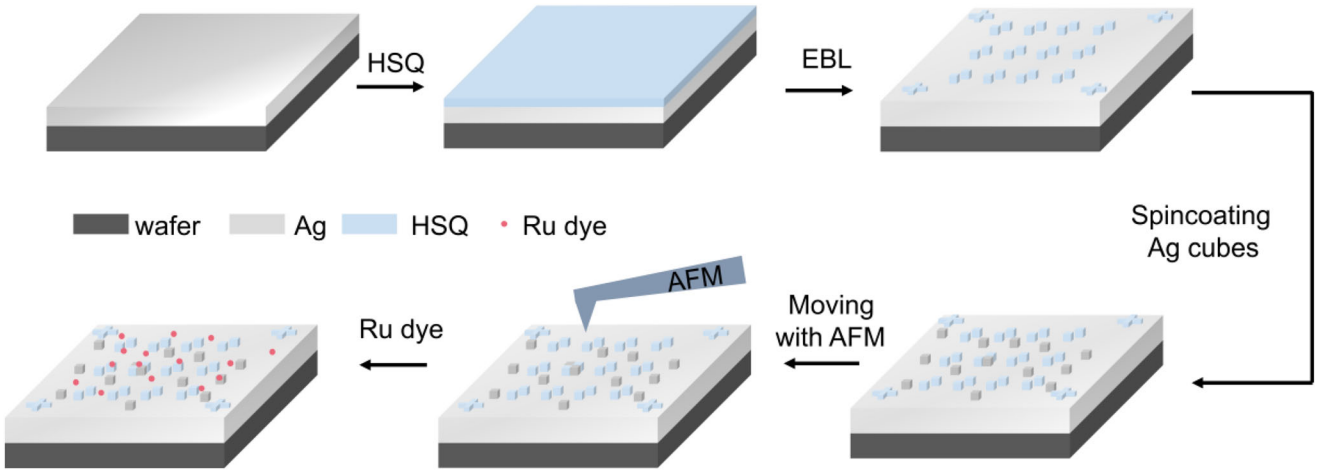

Figure 3. Fabrication process of the coupled system, that is, Ru dye molecules assembled together with Ag nanocube dimers.

(e.g., on the glass, both the concentration and laser power should be high). Decay rate curves are measured by taking histograms of the time interval between a laser sync pulse to a detection event on an avalanche photodiode (APD), using an electronic timing equipment (Picoquant, PicoHarp 300) in a start-stop configuration. As references, the lifetimes of Ru dye molecules on glass and Ag film substrates are measured being 91.7 ns and 126.7 ns, respectively (**Figure 5**a). The difference in lifetimes is mainly caused by the difference in the local density of optical states for different positions and orientations of Ru dye molecules on the two surfaces. In particular, an increase in lifetime for dipoles parallel to the surface of a metallic film happens due to the formation of an image dipole that reduces the strength of the dipole emission, and therefore a suppression of emission is observed,[46] thus experimentally once the molecules form a few-nanometer layer on the silver film, the lifetime may increase comparing with

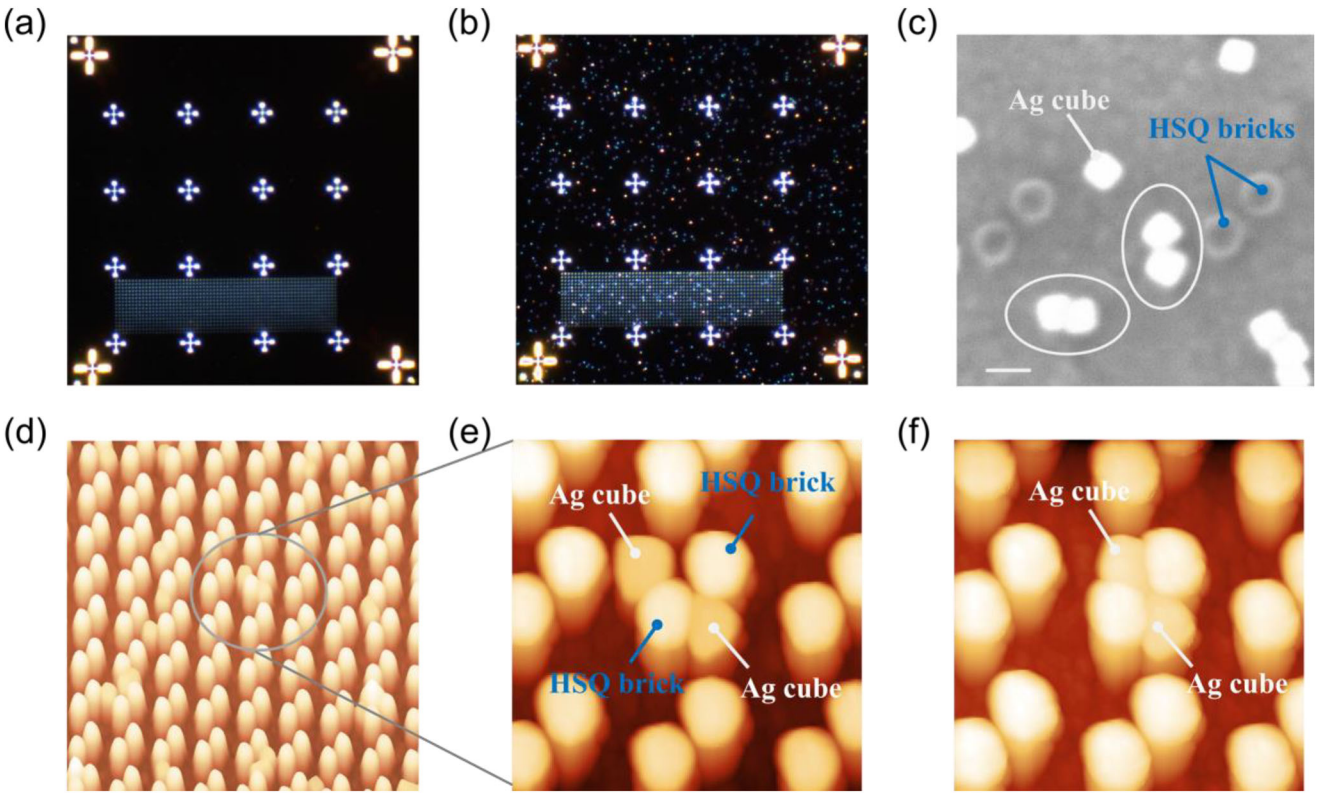

Figure 4. Assembling of Ag nanocube dimers. a) Dark field microscope image of fabricated HSQ bricks and markers. b) Dark field microscope image, taken after spin-coating Ag cubes. c) SEM image of Ag cubes and HSQ bricks. The scale bar, 200 nm. d) AFM image of the area with Ag cubes and HSQ bricks before moving with AFM. e) Zoom-in image of the focused area in (d). f) Ag cubes after their movement by an AFM tip.

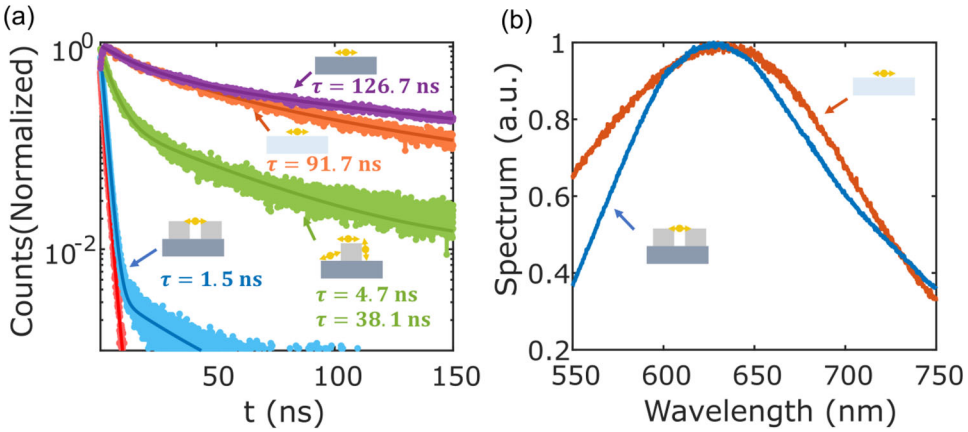

Figure 5. Experimental demonstration of SE enhancement of Ru dye molecules when coupled to Ag nanocube dimers. a) Life-time measurement of Ru dye molecules on Ag film substrate, glass substrate, coupled with single Ag cube, coupled with Ag nanocube dimers. b) Spectra of Ru dye molecules on glass substrate and when coupled with Ag nanocube dimers.

that on the glass substrate. When coupling with individual Ag cubes, the lifetime decreases. By fitting the measured data, with two exponential decay curves, the lifetimes obtained are 4.7 ns and 38.1 ns, which mainly result from the different positions of molecules on the Ag cube, resulting in more than one coupling regime. The dominant part of the lifetime decreases to 1.5 ns when measured for Ru dye molecules coupled with the Ag cube dimer. It should be noted that this lifetime measurement has reached the instrument response function (≈1.5 ns) limit. Therefore, the Purcell enhancement is larger than 61 times when compared to Ru dye molecules on a glass substrate, which experimentally demonstrates the large Purcell enhancement of the designed configuration. We note that this is a lower bound for the Purcell enhancement as the lifetime measured for molecules in dimer cavities reached the IRF limit. From the spectra shown in Figure 5b, the emission peaks of Ru dye molecules are around 630 nm before and after coupling with the designed configuration. It should be noted that this configuration can also be applied to other kinds of QEs with different initial lifetimes and emission wavelengths by appropriately changing the size of Ag cubes.

3. Conclusion

In summary, we propose a configuration consisting of corner-to-corner Ag cube dimers on silver substrates for realizing ultra-large SE enhancement. We investigated the influence of the cube size and the gap distance on the Purcell enhancement, showing that the Purcell factor can reach 6.4×10^6 for the targeted wavelength (630 nm, Ru dye emission peak). Furthermore, we presented an approach for experimentally realizing the proposed configuration with the help of AFM and prefabricated HSQ brick dimers. We show that the lifetime of Ru dye molecules drastically decreases to reach the instrument response function limit (1.5 ns) when coupled to the Ag cube dimer, which demonstrates more than 61 times Purcell enhancement compared to that on glass substrate. We expect that this design and realization approach will make a new avenue for designing advanced quantum light sources with extremely large decay rates.

Acknowledgements

The authors acknowledge the support from National Natural Science Foundation of China (Grant No. 62105150), European Union's Horizon Europe research and innovation programme under the Marie Skłodowska-Curie Action (Grant agreement No. 101064471), Natural Science Foundation of Jiangsu Province (BK20210289), State Key Laboratory of Advanced Optical Communication Systems Networks of China (2022GZKF023), Villum Kann Rasmussen Foundation (Award in Technical and Natural Sciences 2019), and Villum Experiment from Villum Fonden (Grant No. 35950).

Author Contributions

S.K. and Y.H.K. conceived the idea. Y.H.K. performed theoretical modeling and fabricated samples. Y.H.K. and S.K. performed experimental measurement. Y.H.K., S.K., and S.I.B. analyzed the data. S.K. and S.I.B. supervised the project. Y.H.K. wrote the manuscript with contributions from all authors.

Conflict of Interest

The authors declare no conflict of interest.

Data Availability Statement

The data that support the findings of this study are available from the corresponding author upon reasonable request.

Keywords

nanocube dimer, Purcell enhancement, quantum emitter, quantum nanophotonics, spontaneous emission

Received: June 30, 2023
Revised: August 28, 2023
Published online: October 3, 2023

[1] S. Noda, M. Fujita, T. Asano, *Nat. Photonics* **2007**, *1*, 449.
[2] H. J. Kimble, *Nature* **2008**, *453*, 1023.

[3] T. H. Taminiau, F. D. Stefani, F. B. Segerink, N. F. Van Hulst, *Nat. Photonics* **2008**, *2*, 234.
[4] A. Huck, S. Kumar, A. Shakoor, U. L. Andersen, *Phys. Rev. Lett.* **2011**, *106*, 096801.
[5] J. Wang, F. Sciarrino, A. Laing, M. G. Thompson, *Nat. Photonics* **2020**, *14*, 273.
[6] L. Novotny, B. Hecht, *Principles of Nano-Optics*, 2nd ed.; Cambridge University Press, Cambridge **2012**.
[7] A. I. Fernández-Domínguez, S. I. Bozhevolnyi, N. A. Mortensen, *ACS Photonics* **2018**, *5*, 3447.
[8] L. Martín-Moreno, F. J. G. De Abajo, F. J. García-Vidal, *Phys. Rev. Lett.* **2015**, *115*, 173601.
[9] I. Aharonovich, D. Englund, M. Toth, *Nat. Photonics* **2016**, *10*, 631.
[10] S. Kumar, S. I. Bozhevolnyi, *ACS Photonics* **2021**, *8*, 3119.
[11] R. Beams, D. Smith, T. W. Johnson, S.-H. Oh, L. Novotny, A. N. Vamivakas, *Nano Lett.* **2013**, *13*, 3807.
[12] M. Pelton, *Nat. Photonics* **2015**, *9*, 427.
[13] J. N. Farahani, D. W. Pohl, H.-J. Eisler, B. Hecht, *Phys. Rev. Lett.* **2005**, *95*, 017402.
[14] A. F. Koenderink, *Opt. Lett.* **2010**, *35*, 4208.
[15] S. Checcucci, P. Lombardi, S. Rizvi, F. Sgrignuoli, N. Gruhler, F. B. Dieleman, F. S Cataliotti, W. H. Pernice, M. Agio, C. Toninelli, *Light: Sci. Appl.* **2017**, *6*, e16245.
[16] A. F. Koenderink, *ACS Photonics* **2017**, *4*, 710.
[17] J. T. Hugall, A. Singh, N. F. Van Hulst, *ACS Photonics* **2018**, *5*, 43.
[18] M. Frimmer, Y. Chen, A. F. Koenderink, *Phys. Rev. Lett.* **2011**, *107*, 123602.
[19] J. J. Baumberg, J. Aizpurua, M. H. Mikkelsen, D. R. Smith, *Nat. Mater.* **2019**, *18*, 668.
[20] N. Livneh, M. G. Harats, S. Yochelis, Y. Paltiel, R. Rapaport, *ACS Photonics* **2015**, *2*, 1669.
[21] S. I. Bozhevolnyi, J. B. Khurgin, *Optica* **2016**, *3*, 1418.
[22] S. I. Bogdanov, O. A. Makarova, X. Xu, Z. O. Martin, A. S. Lagutchev, M. Olinde, D. Shah, S. N. Chowdhury, A. R. Gabidullin, I. A. Ryzhikov, I. A. Rodionov, A. V. Kildishev, S. I. Bozhevolnyi, A. Boltasseva, V. M. Shalaev, J. B. Khurgin, *Optica* **2020**, *7*, 463.
[23] J. Zhang, Y. Fu, M. H. Chowdhury, J. R. Lakowicz, *Nano Lett.* **2007**, *7*, 2101.
[24] R. Chikkaraddy, X. Zheng, F. Benz, L. J. Brooks, B. De Nijs, C. Carnegie, M.-E. Kleemann, J. Mertens, R. W. Bowman, G. A. E. Vandenbosch, V. V. Moshchalkov, J. J. Baumberg, *ACS Photonics* **2017**, *4*, 469.
[25] S. Kumar, S. K. H. Andersen, S. I. Bozhevolnyi, *ACS Photonics* **2019**, *6*, 23.
[26] G. Zhang, S. Jia, Y. Gu, J. Chen, *Laser Photonics Rev.* **2019**, *13*, 1900025.
[27] S. Kumar, S. I. Bozhevolnyi, *Adv. Quantum Technol.* **2021**, *4*, 2100057.
[28] S. Liu, A. Vaskin, S. Addamane, B. Leung, M.-C. Tsai, Y. Yang, P. P. Vabishchevich, G. A. Keeler, G. Wang, X. He, Y. Kim, N. F. Hartmann, H. Htoon, S. K. Doorn, M. Zilk, T. Pertsch, G. Balakrishnan, M. B. Sinclair, I. Staude, I. Brener, *Nano Lett.* **2018**, *18*, 6906.
[29] S. Kumar, C. Wu, D. Komisar, Y. Kan, L. F. Kulikova, V. A. Davydov, V. N. Agafonov, S. I. Bozhevolnyi, *J. Chem. Phys.* **2021**, *154*, 044303.
[30] Y. Kan, S. I. Bozhevolnyi, *Adv. Opt. Mater.* **2023**, *11*, 2202759.
[31] Y. Kan, S. K. H. Andersen, F. Ding, S. Kumar, C. Zhao, S. I. Bozhevolnyi, *Adv. Mater.* **2020**, *32*, 1907832.
[32] D. Komisar, S. Kumar, Y. Kan, C. Wu, S. I. Bozhevolnyi, *ACS Photonics* **2021**, *8*, 2190.
[33] Y. Kan, F. Ding, C. Zhao, S. I. Bozhevolnyi, *ACS Photonics* **2020**, *7*, 1111.
[34] A. Kinkhabwala, Z. Yu, S. Fan, Y. Avlasevich, K. Müllen, W. E. Moerner, *Nat. Photonics* **2009**, *3*, 654.
[35] G. M. Akselrod, C. Argyropoulos, T. B. Hoang, C. Ciracì, C. Fang, J. Huang, D. R. Smith, M. H. Mikkelsen, *Nat. Photonics* **2014**, *8*, 835.
[36] A. Rose, T. B. Hoang, F. Mcguire, J. J. Mock, C. Ciracì, D. R. Smith, M. H. Mikkelsen, *Nano Lett.* **2014**, *14*, 4797.
[37] T. B. Hoang, G. M. Akselrod, M. H. Mikkelsen, *Nano Lett.* **2016**, *16*, 270.
[38] T. B. Hoang, G. M. Akselrod, C. Argyropoulos, J. Huang, D. R. Smith, M. H. Mikkelsen, *Nat. Commun.* **2015**, *6*, 7788.
[39] S. I. Bogdanov, M. Y. Shalaginov, A. S. Lagutchev, C.-C. Chiang, D. Shah, A. S. Baburin, I. A. Ryzhikov, I. A. Rodionov, A. V. Kildishev, A. Boltasseva, V. M. Shalaev, *Nano Lett.* **2018**, *18*, 4837.
[40] R. Chikkaraddy, B. De Nijs, F. Benz, S. J. Barrow, O. A. Scherman, E. Rosta, A. Demetriadou, P. Fox, O. Hess, J. J. Baumberg, *Nature* **2016**, *535*, 127.
[41] C. Zhang, J.-P. Hugonin, J.-J. Greffet, C. Sauvan, *ACS Photonics* **2019**, *6*, 2788.
[42] R. Faggiani, J. Yang, P. Lalanne, *ACS Photonics* **2015**, *2*, 1739.
[43] J. Cui, S. Koley, Y. E. Panfil, A. Levi, N. Waiskopf, S. Remennik, M. Oded, U. Banin, *Angew. Chem., Int. Ed.* **2021**, *60*, 14467.
[44] S. K. H. Andersen, S. Kumar, S. I. Bozhevolnyi, *Nano Lett.* **2017**, *17*, 3889.
[45] Y. Ma, J. Li, M. Cada, Y. Bian, Z. Han, Y. Ma, M. Iqbal, J. Pištora, *IEEE J. Sel. Top. Quantum Electron.* **2021**, *27*, 4600307.
[46] S. K. H. Andersen, S. Bogdanov, O. Makarova, Y. Xuan, M. Y. Shalaginov, A. Boltasseva, S. I. Bozhevolnyi, V. M. Shalaev, *ACS Photonics* **2018**, *5*, 692.